Impact of urban pressure on the spatial and temporal dynamics of PAH fluxes in an urban tributary of the Seine River (France)

Claire Froger, Cécile Quantin, Johnny Gasperi, Emilie Caupos, Gaël Monvoisin, O. Evrard, Sophie Ayrault

Impact of urban pressure on the spatial and temporal dynamics of PAH fluxes in an urban tributary of the Seine River (France)

Claire Froger*[,1,2], Cécile Quantin[2], Johnny Gasperi[3], Emilie Caupos[3], Gaël Monvoisin[2], Olivier Evrard[1], Sophie Ayrault[1]

Claire Froger

*Corresponding author:
Email: claire.froger@outlook.com
Phone: +33 169824357
Address: Bat. 714, Orme des Merisiers, 91191, Gif-sur-Yvette, France

[1] Laboratoire des Sciences du Climat et de l'Environnement (LSCE/IPSL), CEA-CNRS-UVSQ, Université Paris-Saclay, 91198 Gif-sur-Yvette, France

[2] Géosciences Paris Sud (GEOPS), Université Paris-Sud – CNRS - Université Paris-Saclay, 91400 Orsay, France

[3] Laboratoire Eau Environnement et Systèmes Urbains (LEESU), Université Paris-Est Créteil, UMR MA 102- Agro ParisTech, 94010 Créteil, France

Abstract

Polycyclic aromatic hydrocarbons (PAHs) produced by numerous anthropogenic activities are ubiquitous in the environment and have become a priority concern due to their potential severe biological impacts. A better understanding of PAH transfer at the catchment scale is

therefore necessary to improve the management of PAH contaminants and protect rivers. Furthermore, the impact of changes in hydrological regimes and land uses on PAH fluxes should be specifically investigated. Accordingly, the current research monitors the contamination in atmospheric fallout, soils and rivers in a 950-km^2 catchment (Orge River) characterized by an increasing urban gradient in downstream direction. During an entire hydrological year, river water contamination was quantified through regular sampling of both particulate and dissolved material at four river-monitoring stations, reflecting the increasing urbanization gradient. The significant input of PAHs from urban areas in downstream river sections corresponded to a specific PAH flux that reached 23 g km^{-2} y^{-1} despite the low sediment yield. Moreover, the comparison with runoff-specific fluxes reported in the literature underlined the major impact of urban runoff on the Orge River water and sediment quality. Nevertheless, the annual PAH load exported by the river (21 kg y^{-1}) remained lower than the PAH inputs from atmospheric fallout (173 kg y^{-1}), demonstrating the continuous accumulation of PAH from atmospheric fallout in the catchment soils. Consequently, the notably large PAH stock (close to 1000 tons) resulting from historical contamination of this early-industrialized region continues to increase due to ongoing atmospheric inputs.

Keywords: Urban runoff, PAH mass balance, atmospheric fallout, hydrological regime

1. Introduction

Urban sprawl and human activities have led to deleterious impacts on aquatic ecosystems, with systematic modification of the hydrology, biodiversity, and chemical quality of rivers referred to as “urban river syndrome” (Walsh et al., 2005). Organic contaminants such as polycyclic aromatic hydrocarbons (PAHs), which are released by incomplete combustion or pyrolysis of organic matter, have been targeted by environmental and health public agencies

since the 1970s due to their mutagenicity and carcinogenicity (Grimmer, 1985). Increasing concerns associated with the potential public health problems generated by widespread contamination with these substances has led to the implementation of policies and regulations to control the release of these hazardous compounds. In the European Union, the Water Framework Directives (WFD, Directive 2000/60/EC) requires all member states to adopt environmental measures for water bodies to reach a good ecological and chemical status. In France, the Seine River basin offers an emblematic example of contaminated areas, showing high PAH concentrations in rivers (up to 20 mg kg^{-1} in river-transiting particles) (Fernandes et al., 1997; Uher et al., 2016) and complicating the achievement of good quality targets to such a large extent that the lowest quality grade in 2011 was attributed to the Seine River for those priority pollutants, including PAHs (Fisson et al., 2014).

Awareness of PAH impacts and their regulation occurred after two centuries of continuous release into the Western European atmosphere (Fernández et al., 2000), despite a decrease during the last several decades (Pacyna et al., 2003). This legacy deposition since the industrial revolution resulted in the accumulation of significant PAH stocks in the soils of the Seine River basin (Gaspéri et al., 2018; Gateuille et al., 2014a) as well as in other regions of Europe (Błońska et al., 2016; Jones et al., 1989). Soils are exposed to erosion processes (Lorgeoux et al., 2016; Rose and Rippey, 2002) that might supply PAH-contaminated particles to the rivers (Liu et al., 2013). Moreover, soils are currently exposed to additional PAH contamination sources originating from application of urban sewage sludge (Blanchard et al., 2007), direct vehicular exhaust gases (Gateuille et al., 2014b) and global atmospheric fallout associated with long-range transport of PAHs (Sofowote et al., 2011). The latter might be composed of PAHs originating from remote sources (Ding et al., 2007; Guzzella et al., 2016), local sources of vehicle exhaust emissions (Markiewicz et al., 2017; Oliveira et al., 2011), household heating (Motelay-Massei et al., 2004; Rocher et al., 2004) or industrial

inputs (Cetin et al., 2017; Motelay-Massei et al., 2007). Once deposited on the soil surface, PAHs can be transferred to the aquatic environments by soil erosion processes and runoff on impervious surfaces (Bomboi and Hernández, 1991; Krein and Schorer, 2000). In addition to atmospheric deposition, contaminated particles might be leached from urban surfaces (e.g., from tires and roadway wears) before reaching water bodies (Van Metre et al., 2000). These complex transfer patterns among the atmosphere, soils and rivers are affected by land use and particularly by the occurrence of urban areas, which concentrate multiple PAH sources (Chalmers et al., 2007).

Numerous studies have improved our knowledge of PAH transfers in the environment although they separately addressed the atmosphere (Azimi et al., 2005), soils (Motelay-Massei et al., 2004), river water (Uher et al., 2016), and sediment (Liu et al., 2013). In contrast, few studies have investigated the global contamination at the catchment scale by integrating the atmosphere-soil-river continuum to assess the transfer of these contaminants and their persistence (Gateuille et al., 2014a; Rodenburg et al., 2010). Accordingly, few studies consider the spatial and temporal dynamics of PAH inputs and outputs at the catchment scale. Moreover, most of the available studies that estimate PAH loads supplied by urban areas only covered rather small surface areas (<1-300 ha) (Bressy et al., 2011; Hannouche et al., 2017). For larger catchments, identification of PAH inputs from urban areas was complicated by the remobilization of sediment stored in the channel (Schwientek et al., 2017). Therefore, additional research is needed to quantify both the supply and the signature of PAHs from urban areas to rivers.

The main objective of this study was to calculate the mass balance of PAH (inputs, exports and stocks) in a catchment affected by urban sprawl with a focus on the dynamics of riverine exports through sampling of river water and sediment during contrasting hydrological conditions. Based on this monitoring, the residence time of PAHs in the catchment was

estimated to supply new insights into the persistence of these contaminants in urban areas under temperate climate conditions.

To conduct the current research, a contaminated subcatchment of the Seine River basin, the Orge River (Froger et al., 2018; Le Pape et al., 2012), was selected based on its characteristics, which are similar to those of the Seine River, with a high urban pressure (up to 5,000 inhabitants per km^2 for the Orge catchment at the outlet vs. approximately 8,000 inhabitants per km^2 in the vicinity of Paris megacity). This catchment shows an increasing urbanization gradient in the downstream direction at the expense of cropland and forest. Wastewaters collected in the catchment are drained by a separate sewer to a treatment plant located in a nearby catchment, thus restricting the residential sources to run-off on urban areas, although limited discharges of untreated wastewater to the river might be caused by misconnections. These conditions offer an ideal site with which to investigate potential changes in PAH fluxes in response to urban sprawl and hydrological conditions.

2. Materials and methods

2.1. Study site

The study was conducted in the Orge River catchment, located 30 km south of Paris City (Fig. 1; additional details can be found in Froger et al., (2018)). Three sampling sites were selected on the main stream of the Orge River, and a fourth site was located on its main tributary, the Yvette River. The proportion of urban areas strongly increases in the downstream direction, from 1% in the upper catchment to 56% at the outlet, and the proportion of agricultural lands decreases from 86% to 33% (Table S1). This change is reflected by the increase in population densities in the drainage areas of the monitoring stations, from 300 inhabitants per km^2 at the

most rural study site of Dourdan ("D"), to 5,000 inhabitants per km^2 at Viry ("V", near the outlet).

The geology of the catchment is characterized by Eocene formations, including carbonate rocks, marls and gypsum, and Oligocene formations dominated by Fontainebleau sands (Le Pape et al., 2012).

2.2. Hydrological conditions

Five river water sampling campaigns were conducted from January to December 2016, those campaigns were organized to be as representative as possible of the various hydrological conditions observed in the river. During this period, water discharge measured at the outlet varied from 1.6 to 39.7 $m^3 s^{-1}$ with a mean of 3.5 $m^3 s^{-1}$ (Table S2). The sampling campaigns were organized to be representative of those hydrological conditions observed throughout the year in the Orge River (Fig. 2). Accordingly, each campaign was associated with a water flow class (Fig. 2). One campaign was organized during the low flow period (discharge < 2 $m^3 s^{-1}$ at the outlet), three campaigns during the mean water flow periods (2-5 $m^3 s^{-1}$) and one campaign during high water flow (exceeding 5 $m^3 s^{-1}$). Water samples were also collected on June 06, 2016 at every site (discharge of 15 $m^3 s^{-1}$), during decrease of the water flow of June 2016 exceptional flood extending from 05/29/2016 to 06/10/2016 (with water flow above 10 $m^3 s^{-1}$).

2.3. Sampling and PAH analysis

2.3.1. River and atmospheric deposition sampling

First, suspended particulate matter (SPM) was collected using sediment traps composed of metal bottles submerged in the river were deployed during 4 to 5 days to collect SPM by sedimentation for a longer period (n = 22). Suspended particulate matter recovered from the traps was decanted, the supernatant was removed and the suspended solid was finally freeze-dried (Gateuille et al., 2014a). Samples of SPM collected using sediment traps were demonstrated as representative of suspended particles transported in the river, with PAH contamination levels similar to those of SPM collected by punctual sampling (Bartsch et al., 1996; Gateuille et al., 2014a).

In addition, punctual samples of river water were collected before and after each sediment traps installation (n = 32), using 2-L brown glass bottles preliminarily washed with detergent (TFD4) and heated at 500°C. Extraction of dissolved PAH was rapidly conducted on the samples on the same day as the sample collection.

Suspended particulate matter concentrations were measured by filtering the two punctual bulk water samples collected during each campaign at each site, as well as two additional samples of 10 liters of river water, which provided four SPM estimations for each campaign. During the flood of June 2016 (Figure 2), punctual SPM samples (n = 4) were collected on 06/06/2016 to measure SPM content at each site.

Samples of total atmospheric fallout were collected near the Yvette monitoring site, in Orsay, from February 1, 2016 to March 30, 2017 (Fig. 1). Two funnels with 21 and 28 cm diameters were installed and connected to brown glass bottle collectors. Atmospheric fallout samples (n = 26) were collected after variable periods (median: 16 days) depending on the amount of precipitation.

2.3.2. Sample preparation

The full analytical protocol (i.e, quantification method, and validation using certified material) used in previous studies (Bressy et al., 2012, 2011; Lorgeoux et al., 2016) is detailed in the supplementary material. In brief, instantaneous samples of river water and atmospheric fallout were filtered immediately after sampling, first on quartz filters GF/D (porosity of 2.7 µm) and subsequently on GF/F (pore size of 0.47 µm) previously heated at 500°C. The filters were eventually freeze-dried. Following filtration, extraction was conducted using a solid-phase siliceous cartridge C18 (6 mL and 2000 mg). Solid sample extraction (atmospheric particles, SPM on filters and from sediment traps) was performed using microwave-assisted extraction (Microwave 3000, Anton Paar). Samples were introduced in closed bottles with a mixture of dichloromethane and methanol and heated at 100°C for 10 minutes (Lorgeoux et al., 2016). To avoid interference during the analysis, purification of all extracted samples was performed using silica gel columns (2.1 g of silica gel) to separate the different compound families using various solvent mixtures. Prior to extraction, an internal standard containing 6 deuterated PAHs (naphthaleneD8, acenaphtheneD10, phenanthreneD10, pyreneD12, chryseneD12 and peryleneD12) was added to each sample, both in dissolved and particulate forms. The method was validated based on analyses of certified material (lake sediment standard NIST 1944).

2.3.3. PAH analysis

PAH concentrations in the dissolved and particulate phases of river water samples and atmospheric fallout were measured by gas chromatography coupled with a mass spectrometer (GC-MS, column RTX5SIL-MS (Restek, 60 m, 0.25 mm ID, 0.25 µm df)) used in selected-

ion monitoring mode (see Suppl. Material for details). Helium was the vector gas, the injection volume was 1 µL, and the samples were heated at 330°C for 6 minutes before analysis. The following PAH were measured: fluorene (Fl), phenanthrene (Phe), anthracene (Ant), fluoranthene (Flh), pyrene (Py), benzo(a)anthracene (BaA), chrysene (Chry), benzo(b)fluoranthene (BbF), benzo(k)fluoranthene (BkF), benzo(a)pyrene (BaP), indeno(1,2,3-cd)pyrene (IndP), dibenzo(a,h)anthracene (DbahA) and benzo(g,h,i)perylene (BghiP). The results were expressed as the sum of 13 PAHs. The results found for naphthalene, acenaphthylene and acenaphthene were not considered in the current research because these compounds are too volatile to be correctly quantified (Sicre et al., 2008).

2.4. Flux calculations

2.4.1. Daily riverine export

Daily fluxes of PAH exported by the Orge River were calculated based on Eqs. 1 and 2.

$$\Phi_{part.,I,S} = [PAH]_{part.I,S} \times [SPM]_{I,S} \times Q_{river,IS} \quad (1)$$

$$\Phi_{diss.I,S} = [PAH]_{diss,I,S} \times Q_{river,IS} \quad (2)$$

where $\Phi_{part,I,S}$ and $\Phi_{diss,I,S}$ are the respective daily exports of the particulate and dissolved phases for campaign *I* in g d^{-1} at the site *S*; $[PAH]_{part.I,S}$ is the concentration of PAH in g t^{-1} in the suspended particulate matter; $[PAH]_{diss,I,S}$ is the PAH concentration in the dissolved phase in g m^{-3}; $[SPM]_{I,S}$ is the total suspended matter concentration in t m^{-3} measured during campaign *I* for site *S*; and $Q_{river,I,S}$ is the mean flow rate for site *S* during campaign *I* in m^{-3} d^{-1}. Fluxes were estimated using the median values of $[PAH]_{part,I,S}$, $[SPM]_{I,S}$ and $[PAH]_{diss,I,S}$. Accordingly, the mean values of $\Phi_{part,I,S}$ and $\Phi_{diss,I,S}$ and their respective standard deviations were quantified.

2.4.2. Annual fluxes

2.4.2.1. Atmospheric deposition

The PAH annual deposition is calculated using Eq. 3.

$$\Phi_{an.dep} = \frac{\sum_{i=1}^{n} TAD}{\sum_{i=1}^{n} NbD \times S_{RG}} \times 365 \quad (3)$$

where $\Phi_{an.\ dep}$ is the annual PAH deposition in µg m^{-2} y^{-1}; ΣTAD is the sum of the total atmospheric deposition of the i^{th} sample in µg; ΣNbD is the number of days between successive collections corresponding to the i^{th} sample; and S_{RG} is the surface area of the rainfall collector in m^2.

2.4.2.2. Riverine export

The mean annual flux exported with each fraction (dissolved and particulate) was calculated based on two types of equations: (1) based on data varying according to the hydrological regime and (2) using the SPM and PAH median concentrations. The combination of those estimations offers insight into the impact of the temporal variability of SPM and PAH measurements on the PAH final export.

The first set of equations (Eqs. 4 and 5) involves classification of the hydrological conditions (low, mean, high water flow periods and the extreme flood of June 2016), as described above (Section 2.2, Fig. 2).

$$\Phi_{part,1,S} = \sum_{i=1}^{n}([PAH]_{part,c,S} \times [SPM]_{c,S} \times Q_{i,c,S}) \quad (4)$$

$$\Phi_{diss,1,S} = \sum_{i=1}^{n}([PAH]_{diss,c,S} \times Q_{i,c,S}) \quad (5)$$

The annual PAH exports by the particulate phase $\Phi_{part.1,S}$ and the dissolved phase $\Phi_{diss.1,S}$ in g $year^{-1}$ at each site S were calculated as the sum of the fluxes estimated for each *i* day in g d^{-1}.

The daily flux was calculated using the median $[PAH]_{part,c,S}$ in g t^{-1}, $[SPM]_{c,S}$ in t m^{-3} and $[PAH]_{diss,c,S}$ in g m^{-3} from those campaigns corresponding to each water flow class *c* (defined in Section 2.2) and daily water flow $Q_{i,c,S}$ in m^3 d^{-1} continuously measured near each sampling site. To estimate PAH export during the flood of June 2016 (from 05/29/2016 to 06/10/2016), [SPM] measured at each site on 06/06/2016 and $[PAH]_{part,c,S}$ corresponding to high water flow periods were used.

The second set of equations (Eqs. 6 and 7) used to estimate the PAH riverine fluxes is based on the median concentrations of PAH and SPM for each site:

$$\Phi_{part,2,S} = \sum_{i=1}^{n}([PAH]_{part,med,S} \times [SPM]_{med,S} \times Q_{i,S}) \quad (6)$$

$$\Phi_{diss,2,S} = \sum_{i=1}^{n}([PAH]_{diss,med,S} \times Q_{i,S}) \quad (7)$$

The annual PAH fluxes $\Phi_{part.2,S}$ and $\Phi_{diss.2,S}$ in g y^{-1} correspond to the sum of the *i* daily fluxes at each site *S*. Those fluxes were calculated using the median PAH concentrations and suspended particulate concentrations $[PAH]_{part,med,S}$, $[PAH]_{diss,med,S}$ and $[SPM]_{med,S}$ expressed respectively in µg g^{-1}, ng L^{-1} and mg L^{-1}. For the exceptional flood of June 2016 (05/29/2016 – 06/10/2016), [SPM] measured the 06/06/2016 were used.

The mean PAH riverine export at each site S by the particulate phase ($\Phi_{part,S}$) and the associated standard deviation were calculated as the mean value of $\Phi_{part.1,S}$ and $\Phi_{part.2,S}$. The mean annual export by the dissolved phase ($\Phi_{diss,S}$) was calculated from $\Phi_{diss.1,S}$ and $\Phi_{diss.2,S}$.

2.4.2.3. Specific particulate PAH flux

From the mean particulate PAH fluxes calculated using Eq. 4 and 6, specific fluxes were estimated using the drainage area for each subcatchment and used in the following calculation (Eq. 8).

$$\Phi_{Spec,part,S} = \frac{(\Phi_{part,S})}{S_{DC,S}} \quad (8)$$

Therefore, at each site S, the specific particulate PAH flux in g km^{-2} y^{-1} was calculated using the annual particulate PAH export ($\Phi_{part,S}$) in g y^{-1} and the surface area drained at the site S $S_{DC,S}$, in km^2. The calculations made for Viry site were considered to correspond to the total particulate PAH exported by the entire catchment.

2.4.2.4. *Specific sediment yield*

The specific sediment yield was estimated for each sampling site based on Eq. 9:

$$\Phi_{SY,S} = \frac{\sum_{i=1}^{n}([SPM]_{mean,S} \times Q_{i,S})}{SW} \quad (9)$$

The annual specific sediment yield $\Phi_{SY.,S}$ at site *S* in t km^{-2} y^{-1} was calculated as the sum of the daily SPM fluxes based on the mean concentration of SPM at site *S* in mg L^{-1} ($[SPM]_{mean,S}$) based on the measurements conducted during the four campaigns (Figure 2) and the associated flow rate $Q_{i,S}$ at day *i* across the surface of the watershed SW in km^2. For the exceptional flood of June 2016 (05/29/2016 – 06/10/2016), [SPM] measured on 06/06/2016 were used.

2.4.2.5. *PAH stock in soils*

The stock of PAH in soils under the three main land uses found in the study area (forests, cropland and urban areas) was calculated using Eq. 9 based on those PAH concentrations measured in soils (0-10 cm; n = 32) collected across the entire Seine River basin (Gaspéri et al., 2018).

$$Stock = [PAH] \times D_i \times \rho_{soil} \quad (9)$$

where Stock is the PAH stock in soils in mg m^{-2} ; [PAH] is the PAH concentration in mg kg^{-1} (∑13PAHs) of the soils; D_i is the depth fixed to 0.1 m; and ρ_{soil} is the bulk density of a typical soil of the region, i.e., 2000 kg m^{-3} (Gaspéri et al., 2018).

3. Results and discussion

3.1. PAH contents and fluxes

3.1.1. Atmospheric fallout

Atmospheric fallout showed a wide range of variations in PAH (∑13PAHs) contents, with particulate PAHs contents varying from 5 to 93 µg g^{-1} and dissolved concentrations ranging from 30 to 550 ng L^{-1} (Table S6). The mean PAH concentration in the atmospheric deposition samples was 161 ng L^{-1} throughout the sampling period (min-max: 89-2041 ng L^{-1}). Accordingly, the annual flux was estimated as 182 µg m^{-2} y^{-1} and was similar to the PAH atmospheric fallout measured at various locations in Europe (Table 1). Therefore, PAH atmospheric deposition measured at one single site in this study was considered to be representative of PAH atmospheric fallout across the entire Orge River catchment.

During the study period, no significant variation of PAH atmospheric deposition was observed in response to changes in temperature (Fig. S1 and S2 in SI), which contrasts with the results of previous studies showing higher PAH contents in atmospheric fallout collected during colder periods, which is generally attributed to household heating (Garban et al., 2002; Harrison et al., 1996; Motelay-Massei et al., 2003). Moreover, the rise in PAH production observed in winter is accentuated by a shift in the gas/particle distribution occurring at low temperatures and resulting in higher PAH contamination of particles (Kaupp and McLachlan, 1999; J. Liu et al., 2013). The discrepancy between our results and those of previous studies

might be attributed to sampling duration differences (i.e., 2 weeks in this study and 2 to 7 days in previous studies), which do not allow observation of finer temporal variations in PAH atmospheric fallout.

The proportion of PAH bound to particles varied from 16 to 95%, and the highest particulate proportion was observed in the sample with a total PAH concentration of 2041 ng L^{-1}. The increase in particle-bound PAH from the first (February 2016 to July 2016) to the second period (July 2016 to March 2017) was probably due to the change in filtration material used in the current research (GF/F filters alone during period 1 vs. a combination of GF/D and GF/F filters during period 2) leading to a larger quantity of particles collected (9 ± 5 mg L^{-1} for period 1 vs. 22 ± 26 mg L^{-1} for period 2). After this change, the particulate-bound PAH proportion systematically exceeded 50%. However, the PAH molecular composition of atmospheric particles remained stable with the dominance of 4-ring PAHs (51% ± 8%) compared with that of 3- and 5-6-ring compounds, i.e., 22% ± 9% and 27% ± 10% of the total PAH contamination, respectively. Phenanthrene (14%), fluoranthene (21%), pyrene (21%) and benzo(b)fluoranthene (10%) were the PAHs with the highest concentrations found in the particulate phase.

3.1.2. River contamination

The PAH concentrations in the dissolved phase ranged from 11 to 221 ng L^{-1} with a median value of 41 ng L^{-1} (Table 2). In the particulate phase, the PAH concentrations varied from 1.0 to 45.2 µg g^{-1} with a median of 4.6 µg g^{-1}. Based on the suspended matter contents ranging from 2 to 68 mg L^{-1}, depending on the site and the season considered, the estimated total river concentrations of particulate PAHs varied from 29 to 369 ng L^{-1}.

Comparison with river contamination levels reported in the literature (Table 2) showed that the values found in the Orge River (mean: 4.6 µg g^{-1}) remained in the range of values measured in rivers impacted by urbanization (Seine: 5.8 µg g^{-1}; Elbe: 4.7 µg g^{-1}; Moselle: 4.5 µg g^{-1}).

Particulate-bound PAHs supplied 57% of the total contamination (Fig. S3), in agreement with previous studies reporting that 3- to 6-ring PAHs are mainly transported with particles (Heemken et al., 2000; Shi et al., 2007). However, temporal variations in the PAH partition were observed, particularly at the Dourdan and Yvette sites. Furthermore, spatial variations were observed with an increase in particulate contribution in the downstream direction, with the highest particle-bound contribution of 72% found at the outlet at Viry station (Fig. 3b). These variations could not be related to variations in total suspended solid concentrations because SPM concentrations were similar between sites, integrating all campaigns (Dourdan: 14.1 ± 15.5 mg L^{-1}; Egly: 10.9 ± 6.5 mg.L^{-1}; Yvette: 15.5 ± 9.6 mg.L^{-1}; Viry: 10.2 ± 15.8 mg.L^{-1}). Instead, this increase in particulate PAH proportions in the downstream direction was related to the spatial variations of particulate PAH concentrations increasing from 3.3 µg g^{-1} at the Dourdan site to 8.5 µg g^{-1} at the Viry site (Fig. 3d). In addition, temporal variations associated with the change in hydrological conditions were observed (Fig. 3a), with the highest proportion of dissolved PAH observed in April and the lowest observed in January. A similar trend was observed for dissolved PAH concentrations (Fig. 3c) (Kruskal-Wallis test, α <0.05), suggesting that the change in the dissolved phase contamination might explain the temporal variations observed in PAH partitioning because SPM concentrations and particulate-bound PAH showed the absence of temporal variation (Fig. 3c). The higher dissolved PAH concentrations measured during high water flows might be explained by the increase in PAH desorption that occurs when particles are resuspended from the channel bed

and well mixed in the water column during floods (Belles et al., 2016). However, although this increase in surface water contamination in response to flood events has been observed in several studies (Dong et al., 2016; Mouhri et al., 2008), it has not been systematically reported (Gateuille et al., 2014a; Sicre et al., 2008).

3.2. Impact of hydrological conditions on PAH fluxes

The daily riverine exports of dissolved PAHs were estimated based on only four sampling campaigns for the dissolved PAHs (Fig. 2). Detailed values are supplied in the supplementary material. The fluxes of dissolved PAH at the outlet ranged from 6 to 32 g d^{-1}, with the highest load observed during the flood of April 2016 and the lowest load observed during the low stage period of August 2016. Compared with those results obtained for the Seine River, which are characterized by a discharge varying from 100 to 700 m^3 s^{-1} and dissolved PAH fluxes estimated to vary from 690 to 4838 g d^{-1} (PAH concentration of 80 ng L^{-1}), the Orge River supplied 1% of the total dissolved PAH export of the Seine River basin, which remains proportional to its surface (1.3% of the Seine River basin).

Fluxes from each upper subcatchment (i.e., Egly and Yvette) are shown in Fig. 4. Accordingly, the difference between the fluxes calculated for the entire catchment and the upper subcatchment fluxes corresponded to those PAH fluxes supplied by the downstream urban area that is referred to as $Viry_{sub}$ in the remainder of the text. With respect to the subcatchment fluxes, it appears that the main proportion of the dissolved PAH exported at the outlet (Viry) originated from upper catchment portions (i.e., Egly and Yvette subcatchments) because their PAH fluxes were equivalent to those fluxes measured at the outlet, resulting in a budget of +6.0 g d^{-1}, -12.6 g d^{-1}, -0.5 g d^{-1} and -0 2 g d^{-1} for January, April, August and November 2016, respectively. This result demonstrates the absence of significant dissolved

375 PAH supply from the $Viry_{sub}$ subcatchment suggesting that PAH inputs from those urban
376 areas downstream were mainly associated with the particulate phase.

377 In contrast, the temporal variability of particulate PAH fluxes suggests the large impact of
378 seasonal variations of water flow and urbanization on PAH discharge. Accordingly, the
379 highest PAH loads were observed during the flood in April, corroborating the results of
380 previous studies showing a major export of PAH during floods (Conaway et al., 2013; Mouhri
381 et al., 2008). During this flood event, particulate PAH supplied to the lower river section that
382 drains urban areas, i.e., $Viry_{sub}$, reached a maximum of 23.9 g d^{-1}. This result suggests that the
383 downstream portion of the catchment concentrating the majority of the urban areas (Fig. 1)
384 supplied up to 53% of the total PAH exported by the particulate phase in the catchment for
385 this campaign (Table 3). During the moderate water flow periods of January and November
386 2016, the $Viry_{sub}$ loads were 18.9 and 17.0 g d^{-1}, respectively, supplying 62% of the total PAH
387 flux at the outlet (Table 3). A negative export from this urban river section was observed
388 during the low flow period of August 2016, with -4.0 g d^{-1} underlining the notably low supply
389 of PAH from these areas during this campaign.

390 Comparison of the different subcatchment (i.e., Egly, Yvette and $Viry_{sub}$) contributions to the
391 total particulate PAH fluxes clearly shows that $Viry_{sub}$ supplied a significant contribution of
392 PAHs in January, April and November despite the low total sediment load (Table 3). Studies
393 conducted in urban areas reported that PAH contamination in runoff waters was mainly
394 carried by the particulate phase (85%) and that it did not decrease with increasing stormflow,
395 which suggests that urban surfaces supply a constant source of particulate PAH (Gasperi et
396 al., 2009; Hwang and Foster, 2006). These observations are corroborated by the results found
397 in the current research showing that the occurrence of heavy rainfall generated higher runoff
398 volumes in urban areas (e.g., during the flood event in April 2016 and the average discharge

399 conditions campaigns of January and November 2016), thus increasing the PAH load supplied
400 by these areas (Table 3).

401 In contrast to $Viry_{sub}$, the higher sediment yield of the Yvette subcatchment was associated
402 with the lowest contribution to the PAH total export at the outlet (Table 3). This result is
403 likely explained by the construction of an extensive research campus, the Saclay Plateau, in
404 the upper catchment portions, resulting in extensive soil erosion (Chin, 2006; Huon et al.,
405 2017) and the dilution of PAH concentrations by preferential mobilization of uncontaminated
406 subsurface particles. Among the four campaigns, only the survey conducted during the low
407 flow period in August 2016 showed the major contribution of the upper catchment portions to
408 the total PAH export. The negative mass-balance for this campaign could be explained by
409 both sedimentation of particles during their transfer from Egly and Yvette to the outlet and a
410 notably low input from $Viry_{sub}$, insufficient to compensate the deposition of upstream PAH.
411 Finally, the impact of urban runoff on PAH fluxes is particularly clear in the downstream
412 portion of the Orge River catchment because of the channelization of the river section near the
413 outlet. This configuration limits sediment storage and potential dilution of PAH urban loads
414 by particles eroded from less contaminated soils or channel banks (Schwientek et al., 2017,
415 2013).

416

417

418 ### 3.3. Annual mass balance of PAH

419 The annual PAH catchment budget was estimated for 2016 based on PAH concentrations,
420 SPM concentrations, daily water flow and total atmospheric deposition (Fig. 5). First, global
421 accumulation of these compounds was observed. From the 173 kg of PAHs deposited with
422 atmospheric fallout on catchment soils, only 34.5 ± 0.7 kg of PAH were exported by the river,

423 resulting in an accumulation of 80% of the contamination deposited from the atmosphere in
424 the soils (138 kg y^{-1}). A similar result was found for all subcatchments, with an accumulation
425 of 28 kg y^{-1} for the Yvette catchment, 6 kg y^{-1} for the Dourdan catchment, 73 kg y^{-1} for the
426 Egly catchment and 31 kg y^{-1} for $Viry_{sub}$, corresponding to 84%, 87%, 84% and 68% of the
427 respective atmospheric fallout inputs. The PAH accumulation rates are based on the
428 hypothesis of conservation of PAH deposited by atmospheric fallout in soils. This assumption
429 is supported by the higher PAH stability of those 4-to-6 ring PAHs (Biache et al., 2014;
430 Cébron et al., 2013), contributing to 66% of the total atmospheric fallout. A second
431 assumption is that atmospheric deposition is homogenous across the catchment. This later
432 hypothesis is supported by the similar PAH deposition rates measured across Europe and
433 particularly across the entire Paris region (Table 1). The accumulation rates estimated in the
434 current study should be considered as an order of magnitude given the large uncertainties
435 associated with the particle flux estimations and the assumptions made on the PAH behavior.

436 In both atmospheric fallout and riverine exports, the particulate fraction dominated the
437 transport of PAH, especially in the Yvette subcatchment (82% of particulate-bound PAH) and
438 in the lower portions of the catchment ($Viry_{sub}$: 93%). Specific particulate PAH fluxes were
439 calculated, demonstrating that $Viry_{sub}$ was the main source of particulate PAH, with a
440 production of 46.7 ± 2.5 g km^{-2} y^{-1} (Table 4) compared with the total PAH export at the outlet
441 in Viry (28.7 ± 0.1 g km^{-2} y^{-1}) and the Egly and Yvette subcatchments (19.1 ± 1.0 and 24.8 ±
442 0.7 g km^{-2} y^{-1} respectively). Specific PAH fluxes and sediments yields were estimated for a
443 compilation of studies found in the literature (Table 2; Table 4). Annual specific loads found
444 in the current research (28.7 g km^{-2} y^{-1}) were higher than those fluxes reported for the Moselle
445 River (13.1 g km^{-2} y^{-1}), and appeared to be similar to the loads reported for the Orgeval River
446 (30 g km^{-2} y^{-1}), the Elbe River (28.5 g km^{-2} y^{-1}) and the Mackenzie River (27 g km^{-2} y^{-1}).
447 However, among those sites with equivalent PAH specific loads, the rural subcatchments of

448 the Orgeval and Mackenzie Rivers showed a sediment yield 3-fold higher than the other
449 catchments. Despite their lower sediment yields, the urban Orge, Moselle and Elbe River
450 catchments were characterized by relatively high PAH riverine export, reflecting the high
451 contamination levels found in the sediment transiting these low-turbidity rivers. Accordingly,
452 the impact of urban inputs on the contamination of the river can be characterized by a ratio
453 between the PAH specific load (in g km^{-2} y^{-1}) and the sediment yield (in t km^{-2} y^{-1}), resulting
454 in a theoretical PAH concentration in SPM (in $g.t^{-1}$), considering both the anthropogenic
455 pressure and the potential dilution in the river (Table 4). This ratio is similar to the mean
456 particle-bound PAH concentration developed by Schwientek et al., (2017).

457 Consequently, urban catchments, regardless of their drainage surface (i.e., Orge River, Seine
458 River, Moselle River, Körsh River and Elbe River), showed ratios exceeding 4, whereas rural
459 catchments such as the Orgeval River and forested catchments such as the Mackenzie River
460 were characterized by ratios lower than 2. The Rhône River, a mixed catchment that drains
461 dense urban areas (Lyon) as well as large forested and agricultural areas in the upper portions,
462 showed a low ratio of 2.2, explained by the notably high sediment yield (76 t km^{-2} y^{-1}). In the
463 Orge River catchment, this ratio increased with the urbanization gradient in the downstream
464 direction (Dourdan < Yvette < Egly < $Viry_{sub}$), confirming the higher supply of PAHs from
465 urban areas.

466 The ratio of 15 found for $Viry_{sub}$ was similar to that found for precipitation runoff collected in
467 the small urban catchment of Sucy, located south of Paris (Hannouche et al., 2017). This
468 catchment showed characteristics similar to those found in $Viry_{sub}$ (population density of 2500
469 inhabitants per km^2 and dense urban area) with a load ratio of 17 (Table 4). Therefore, the
470 similarities between PAH inputs from $Viry_{sub}$ and those PAH loads from runoff on urban
471 surfaces illustrate the impact of urban runoff on the Orge River quality. These results also
472 suggest that this ratio reflects the impact of both historical and current human activities

supplying contaminants to the river on the sediment quality and might offer a tool for environmental assessment of the anthropogenic pressure on rivers. Based on the data collected in the current research and those reported in the literature (Table 4), a maximum ratio value of 2 is proposed as a threshold to characterize catchments with a low impact of human activities on the river quality. Furthermore, ratio values exceeding 4 are suggested for identification of highly impacted catchments. Nevertheless, to better constrain PAH riverine export, continuous measurements of SPM should be conducted to refine PAH fluxes estimations and specific sediment yields in the catchment.

3.4. Evaluation of PAH stocks in soils depending on land use

Stocks of PAHs in the upper 10-cm layer of the soils were estimated under each land use (Table S8) based on the values measured in a set of soils collected across the Paris areas including the Orge River catchment area (Gaspéri et al., 2018). However, as a large range of PAH concentrations was reported in Gasperi et al. (2018), extreme values (min and max) were also considered when estimating the PAH stock in the soils of the Orge River catchment to evaluate the range of variability of the stock estimate. The application of these values to the soils of the Orge River catchment resulted in a significant stock of PAH in soils (Table 5), with a minimum of 7, 13 and 14 tons of PAHs in urban soils, 13 tons in forest soils, and 14 tons in agricultural soils. Atmospheric fallout of 46, 53 and 74 kg y^{-1} deposited on urban, forested and agricultural soils, appeared to be negligible (<0.01%) compared to the estimated PAH stock in the soils corresponding to each of the three land uses considered (Table 8). These levels of soil contamination are highly likely to be associated with the accumulation of PAH emitted for more than a century by industrial and urban activities in the region

(Lorgeoux et al., 2016; Pacyna et al., 2003). If assuming that the current PAH deposition measured in the current research (i.e., 182 µg m^{-2} y^{-1}) is representative of that observed over the long term, 161 years is expected to accumulate the lowest PAH stock estimated in soils, whereas 61,000 years are required to reach those values found in the most polluted soils. Those estimations suggest that higher PAH atmospheric deposition rates occurred during the late 19th and the early 20th centuries, which corroborates the results of a study conducted in Northern Spain that reported atmospheric deposition rates of up to 2,500 µg m^{-2} y^{-1} in the 1970s (Leorri et al., 2014).

Despite the decrease of long-range atmospheric PAH fallout (Pacyna et al., 2003), the reservoir of legacy PAH contamination in soils is not declining, as demonstrated by the ongoing PAH accumulation observed in 2016 in soils of the Orge River catchment. Significant PAH stocks have also been observed in the soils in rural areas of the Seine River basin, confirming the long term accumulation of PAH in the entire region (Gateuille et al., 2014a). Despite multiple studies demonstrating PAH sensitivity to biodegradation or oxidation processes in soils and rivers (Biache et al., 2014; Haritash and Kaushik, 2009), the PAH stocks found in soils suggest low degradation of PAH in natural environments. Consequently, management of the current PAH contamination in ecosystems should consider the dominance of this legacy contamination and focus on those PAH transfers and pathways to the aquatic system in addition to mitigation of local sources such as vehicular exhaust and household heating.

4. Conclusions

The current study quantified PAH contamination in the atmospheric fallout during an entire year, and the contamination of main rivers of the Orge River catchment based on five

campaigns representative of those hydrological variations observed in this area. Moreover, the temporal variations of the PAH fluxes and those of particulate PAH concentrations demonstrated the significant contribution of urban areas in the lower catchment portions to the particulate PAH export, which primarily occurred during mean and high water flow periods. The ratio of PAH specific fluxes and sediment yields, which was developed in the current research as an indicator of anthropogenic pressure on catchments, confirmed the impact of urbanization on the Orge River. However, despite the large PAH exports from urban areas, PAH continues to accumulate in the catchment soils. Finally, comparison of the current PAH deposition with the estimation of the PAH stock in the catchment soils based on values from the literature suggests that legacy contamination of the soils might act as an extensive source of PAH supplied to the rivers during the next several decades or even centuries. Source apportionment should therefore be conducted to quantify the respective contributions of legacy and contemporary contamination to PAH transiting the rivers. The identification of PAH sources using multiple tracing tools, including PAH diagnostic ratios, might offer further insights into the contamination dynamics in early industrialized catchments and guide the design of effective measures to manage this ubiquitous contamination.

Acknowledgements

This research was financially supported by Paris-Sud University (PhD grant), the ”Initiative de Recherche Stratégique” ACE-ICSEN funded by the University Paris-Saclay and the Seine River research program PIREN-Seine.

References

Azimi, S., Rocher, V., Muller, M., Moilleron, R., Thevenot, D.R., 2005. Sources, distribution and variability of hydrocarbons and metals in atmospheric deposition in an urban area (Paris, France). Sci. Total Environ. 337, 223–239. https://doi.org/10.1016/j.scitotenv.2004.06.020

Bartsch, L. a., Rada, R.G., Sullivan, J.F., 1996. A comparison of solids collected in sediment traps and automated water samplers. Hydrobiologia 323, 61–66. https://doi.org/10.1007/BF00020547

Belles, A., Mamindy-Pajany, Y., Alary, C., 2016. Simulation of aromatic polycyclic hydrocarbons remobilization from a river sediment using laboratory experiments supported by passive sampling techniques. Environ. Sci. Pollut. Res. 23, 2426–2436. https://doi.org/10.1007/s11356-015-5462-y

Biache, C., Mansuy-Huault, L., Faure, P., 2014. Impact of oxidation and biodegradation on the most commonly used polycyclic aromatic hydrocarbon (PAH) diagnostic ratios: Implications for the source identifications. J. Hazard. Mater. 267, 31–39. https://doi.org/10.1016/j.jhazmat.2013.12.036

Blanchard, M., Teil, M.J., Guigon, E., Larcher-Tiphagne, K., Ollivon, D., Garban, B., Chevreuil, M., 2007. Persistent toxic substance inputs to the river Seine basin (France) via atmospheric deposition and urban sludge application. Sci. Total Environ. 375, 232–243. https://doi.org/10.1016/j.scitotenv.2006.12.012

Błońska, E., Lasota, J., Szuszkiewicz, M., Łukasik, A., Klamerus-Iwan, A., 2016. Assessment of forest soil contamination in Krakow surroundings in relation to the type of stand.

Environ. Earth Sci. 75, 1205. https://doi.org/10.1007/s12665-016-6005-7

Bomboi, M.T., Hernández, A., 1991. Hydrocarbons in urban runoff: Their contribution to the wastewaters. Water Res. 25, 557–565. https://doi.org/10.1016/0043-1354(91)90128-D

Bressy, A., Gromaire, M.-C., Lorgeoux, C., Chebbo, G., 2011. Alkylphenols in atmospheric depositions and urban runoff. Water Sci. Technol. 63, 671 LP-679.

Bressy, A., Gromaire, M.-C., Lorgeoux, C., Saad, M., Leroy, F., Chebbo, G., 2012. Towards the determination of an optimal scale for stormwater quality management: Micropollutants in a small residential catchment. Water Res. 46, 6799–6810. https://doi.org/10.1016/j.watres.2011.12.017

Cébron, A., Faure, P., Lorgeoux, C., Ouvrard, S., Leyval, C., 2013. Experimental increase in availability of a PAH complex organic contamination from an aged contaminated soil: Consequences on biodegradation. Environ. Pollut. 177, 98–105. https://doi.org/10.1016/j.envpol.2013.01.043

Cetin, B., Ozturk, F., Keles, M., Yurdakul, S., 2017. PAHs and PCBs in an Eastern Mediterranean megacity, Istanbul: Their spatial and temporal distributions, air-soil exchange and toxicological effects. Environ. Pollut. 220, 1322–1332. https://doi.org/10.1016/j.envpol.2016.11.002

Chalmers, A.T., Van Metre, P.C., Callender, E., 2007. The chemical response of particle-associated contaminants in aquatic sediments to urbanization in New England, U.S.A. J. Contam. Hydrol. 91, 4–25. https://doi.org/10.1016/j.jconhyd.2006.08.007

Chin, A., 2006. Urban transformation of river landscapes in a global context. Geomorphology 79, 460–487. https://doi.org/10.1016/j.geomorph.2006.06.033

Conaway, C.H., Draut, A.E., Echols, K.R., Storlazzi, C.D., Ritchie, A., 2013. Episodic Suspended Sediment Transport and Elevated Polycyclic Aromatic Hydrocarbon Concentrations in a Small, Montainous River in Coastal California. River Res. Appl. 29, 919–932. https://doi.org/10.1002/rra.2582

Delmas, M., Pak, L.T., Cerdan, O., Souchère, V., Le Bissonnais, Y., Couturier, A., Sorel, L., 2012. Erosion and sediment budget across scale: A case study in a catchment of the European loess belt. J. Hydrol. 420–421, 255–263. https://doi.org/10.1016/j.jhydrol.2011.12.008

Ding, X., Wang, X.-M., Xie, Z.-Q., Xiang, C.-H., Mai, B.-X., Sun, L.-G., Zheng, M., Sheng, G.-Y., Fu, J.-M., Pöschl, U., 2007. Atmospheric polycyclic aromatic hydrocarbons observed over the North Pacific Ocean and the Arctic area: Spatial distribution and source identification. Atmos. Environ. 41, 2061–2072. https://doi.org/10.1016/j.atmosenv.2006.11.002

Dong, J., Xia, X., Wang, M., Xie, H., Wen, J., Bao, Y., 2016. Effect of recurrent sediment resuspension-deposition events on bioavailability of polycyclic aromatic hydrocarbons in aquatic environments. J. Hydrol. 540, 934–946. https://doi.org/10.1016/j.jhydrol.2016.07.009

Fernandes, M.B., Sicre, M.-A., Boireau, A., Tronczynski, J., 1997. Polyaromatic hydrocarbon (PAH) distributions in the Seine River and its estuary. Mar. Pollut. Bull. 34, 857–867. https://doi.org/10.1016/S0025-326X(97)00063-5

Fernández, P., Vilanova, R.M., Martínez, C., Appleby, P., Grimalt, J.O., 2000. The Historical Record of Atmospheric Pyrolytic Pollution over Europe Registered in the Sedimentary PAH from Remote Mountain Lakes. Environ. Sci. Technol. 34, 1906–1913.

https://doi.org/10.1021/es9912271

Fisson, C., Bacq, N., Gilles, B., Boust, D., Budzinski, H., Jean, D., Fontaine, T., Garnier, J., Homer, S., Lacroix, J., Leroy, B., Sansom, S., 2014. Qualité des eaux de l'Estuaire de la Seine - Fascicule 3.2.

Foan, L., Domercq, M., Bermejo, R., Santamaría, J.M., Simon, V., 2015. Mosses as an integrating tool for monitoring PAH atmospheric deposition: Comparison with total deposition and evaluation of bioconcentration factors. A year-long case-study. Chemosphere 119, 452–458. https://doi.org/10.1016/j.chemosphere.2014.06.071

Froger, C., Ayrault, S., Evrard, O., Monvoisin, G., Bordier, L., Lefèvre, I., Quantin, C., 2018. Tracing the sources of suspended sediment and particle-bound trace metal elements in an urban catchment coupling elemental and isotopic geochemistry, and fallout radionuclides. Environ. Sci. Pollut. Res. 25, 28667–28681. https://doi.org/10.1007/s11356-018-2892-3

Garban, B., Blanchoud, H., Motelay-Massei, A., Chevreuil, M., Ollivon, D., 2002. Atmospheric bulk deposition of PAHs onto France: trends from urban to remote sites. Atmos. Environ. 36, 5395–5403. https://doi.org/10.1016/S1352-2310(02)00414-4

Gaspéri, J., Ayrault, S., Moreau-Guigon, E., Alliot, F., Labadie, P., Budzinski, H., Blanchard, M., Muresan, B., Caupos, E., Cladière, M., Gateuille, D., Tassin, B., Bordier, L., Teil, M.-J., Bourges, C., Desportes, A., Chevreuil, M., Moilleron, R., 2018. Contamination of soils by metals and organic micropollutants: case study of the Parisian conurbation. Environ. Sci. Pollut. Res. 25, 23559–23573. https://doi.org/10.1007/s11356-016-8005-2

Gasperi, J., Garnaud, S., Rocher, V., Moilleron, R., 2009. Priority pollutants in surface waters

and settleable particles within a densely urbanised area: Case study of Paris (France). Sci. Total Environ. 407, 2900–2908. https://doi.org/10.1016/j.scitotenv.2009.01.024

Gateuille, D., Evrard, O., Lefevre, I., Moreau-Guigon, E., Alliot, F., Chevreuil, M., Mouchel, J.-M., 2014a. Mass balance and decontamination times of Polycyclic Aromatic Hydrocarbons in rural nested catchments of an early industrialized region (Seine River basin, France). Sci. Total Environ. 470–471, 608–617. https://doi.org/10.1016/j.scitotenv.2013.10.009

Gateuille, D., Evrard, O., Lefevre, I., Moreau-Guigon, E., Alliot, F., Chevreuil, M., Mouchel, J.M., 2014b. Combining measurements and modelling to quantify the contribution of atmospheric fallout, local industry and road traffic to PAH stocks in contrasting catchments. Environ. Pollut. 189, 152–160. https://doi.org/10.1016/j.envpol.2014.02.029

Gocht, T., Klemm, O., Grathwohl, P., 2007. Long-term atmospheric bulk deposition of polycyclic aromatic hydrocarbons (PAHs) in rural areas of Southern Germany. Atmos. Environ. 41, 1315–1327. https://doi.org/10.1016/j.atmosenv.2006.09.036

Grimmer, G., 1985. PAH—Their contribution to the carcinogenicity of various emissions†. Toxicol. Environ. Chem. 10, 171–181. https://doi.org/10.1080/02772248509357101

Guzzella, L., Salerno, F., Freppaz, M., Roscioli, C., Pisanello, F., Poma, G., 2016. POP and PAH contamination in the southern slopes of Mt. Everest (Himalaya, Nepal): Long-range atmospheric transport, glacier shrinkage, or local impact of tourism? Sci. Total Environ. 544, 382–390. https://doi.org/10.1016/j.scitotenv.2015.11.118

Hannouche, A., Chebbo, G., Joannis, C., Gasperi, J., Gromaire, M., Moilleron, R., Barraud, S., Ruban, V., 2017. Stochastic evaluation of annual micropollutant loads and their

uncertainities in separate storm sewer. Environ. Sci. Pollut. Res. 1–15.

Haritash, A.K., Kaushik, C.P., 2009. Biodegradation aspects of Polycyclic Aromatic Hydrocarbons (PAHs): A review. J. Hazard. Mater. 169, 1–15. https://doi.org/10.1016/j.jhazmat.2009.03.137

Harrison, R.M., Smith, D.J.T., Luhana, L., 1996. Source apportionment of atmospheric polycyclic aromatic hydrocarbons collected from an urban location in Birmingham, U.K. Environ. Sci. Technol. 30, 825–832 ST–Source apportionment of athmospheric.

Heemken, O.P., Stachel, B., Theobald, N., Wenclawiak, B.W., 2000. Temporal variability of organic micropollutants in suspended particulate matter of the River Elbe at Hamburg and the River Mulde at Dessau, Germany. Arch. Environ. Contam. Toxicol. 38, 11–31. https://doi.org/10.1007/s002449910003

Huon, S., Evrard, O., Gourdin, E., Lefèvre, I., Bariac, T., Reyss, J.-L., Henry des Tureaux, T., Sengtaheuanghoung, O., Ayrault, S., Ribolzi, O., 2017. Suspended sediment source and propagation during monsoon events across nested sub-catchments with contrasted land uses in Laos. J. Hydrol. Reg. Stud. 9, 69–84. https://doi.org/10.1016/j.ejrh.2016.11.018

Hwang, H.-M., Foster, G.D., 2006. Characterization of polycyclic aromatic hydrocarbons in urban stormwater runoff flowing into the tidal Anacostia River, Washington, DC, USA. Environ. Pollut. 140, 416–426. https://doi.org/10.1016/j.envpol.2005.08.003

Jones, K.C., Stratford, J.A., Tidridge, P., Waterhouse, K.S., Johnston, A.E., 1989. Polynuclear aromatic hydrocarbons in an agricultural soil: Long-term changes in profile distribution. Environ. Pollut. 56, 337–351. https://doi.org/10.1016/0269-7491(89)90079-1

Kaupp, H., McLachlan, M.S., 1999. Gas/particle partitioning of PCDD/Fs, PCBs, PCNs and

PAHs. Chemosphere 38, 3411–3421. https://doi.org/10.1016/S0045-6535(98)00554-2

Krein, A., Schorer, M., 2000. Road runoff pollution by polycyclic aromatic hydrocarbons and its contribution to river sediments. Water Res. 34, 4110–4115. https://doi.org/10.1016/S0043-1354(00)00156-1

Le Meur, M., Mansuy-Huault, L., Lorgeoux, C., Bauer, A., Gley, R., Vantelon, D., Montargès-Pelletier, E., 2017. Spatial and temporal variations of particulate organic matter from Moselle River and tributaries: A multimolecular investigation. Org. Geochem. 110, 45–56. https://doi.org/10.1016/j.orggeochem.2017.04.003

Le Pape, P., Ayrault, S., Quantin, C., 2012. Trace element behavior and partition versus urbanization gradient in an urban river (Orge River, France). J. Hydrol. 472–473, 99–110. https://doi.org/10.1016/j.jhydrol.2012.09.042

Leorri, E., Mitra, S., Irabien, M.J., Zimmerman, A.R., Blake, W.H., Cearreta, A., 2014. A 700year record of combustion-derived pollution in northern Spain: Tools to identify the Holocene/Anthropocene transition in coastal environments. Sci. Total Environ. 470–471, 240–247. https://doi.org/10.1016/j.scitotenv.2013.09.064

Liu, J., Li, J., Lin, T., Liu, D., Xu, Y., Chaemfa, C., Qi, S., Liu, F., Zhang, G., 2013. Diurnal and nocturnal variations of PAHs in the Lhasa atmosphere, Tibetan Plateau: Implication for local sources and the impact of atmospheric degradation processing. Atmos. Res. 124, 34–43. https://doi.org/10.1016/j.atmosres.2012.12.016

Liu, Y., Beckingham, B., Ruegner, H., Li, Z., Ma, L., Schwientek, M., Xie, H., Zhao, J., Grathwohl, P., 2013. Comparison of Sedimentary PAHs in the Rivers of Ammer (Germany) and Liangtan (China): Differences between Early- and Newly-Industrialized

Countries. Environ. Sci. Technol. 47, 701–709. https://doi.org/10.1021/es3031566

Lorgeoux, C., Moilleron, R., Gasperi, J., Ayrault, S., Bonté, P., Lefèvre, I., Tassin, B., Bonté, P., Lefèvre, I., Tassin, B., 2016. Temporal trends of persistent organic pollutants in dated sediment cores: Chemical fingerprinting of the anthropogenic impacts in the Seine River basin, Paris. Sci. Total Environ. 541, 1355–1363. https://doi.org/10.1016/j.scitotenv.2015.09.147

Markiewicz, A., Björklund, K., Eriksson, E., Kalmykova, Y., Strömvall, A.-M., Siopi, A., 2017. Emissions of organic pollutants from traffic and roads: Priority pollutants selection and substance flow analysis. Sci. Total Environ. 580, 1162–1174. https://doi.org/10.1016/j.scitotenv.2016.12.074

Motelay-Massei, A., Ollivon, D., Garban, B., Chevreuil, M., 2003. Polycyclic aromatic hydrocarbons in bulk deposition at a suburban site: assessment by principal component analysis of the influence of meteorological parameters. Atmos. Environ. 37, 3135–3146. https://doi.org/10.1016/S1352-2310(03)00218-8

Motelay-Massei, A., Ollivon, D., Garban, B., Teil, M.J., Blanchard, M., Chevreuil, M., 2004. Distribution and spatial trends of PAHs and PCBs in soils in the Seine River basin, France. Chemosphere 55, 555–565. https://doi.org/10.1016/j.chemosphere.2003.11.054

Motelay-Massei, A., Ollivon, D., Garban, B., Tiphagne-Larcher, K., Zimmerlin, I., Chevreuil, M., 2007. PAHs in the bulk atmospheric deposition of the Seine river basin: Source identification and apportionment by ratios, multivariate statistical techniques and scanning electron microscopy. Chemosphere 67, 312–321. https://doi.org/10.1016/j.chemosphere.2006.09.074

Mouhri, A., Motelay-massei, A., Massei, N., Fournier, M., Laignel, B., 2008. Polycyclic aromatic hydrocarbon transport processes on the scale of a flood event in the rural watershed of Le Bebec, France. Chemosphere 73, 443–450. https://doi.org/10.1016/j.chemosphere.2008.05.046

Oliveira, C., Martins, N., Tavares, J., Pio, C., Cerqueira, M., Matos, M., Silva, H., Oliveira, C., Camões, F., 2011. Size distribution of polycyclic aromatic hydrocarbons in a roadway tunnel in Lisbon, Portugal. Chemosphere 83, 1588–1596. https://doi.org/10.1016/j.chemosphere.2011.01.011

Ollivon, D., Garban, B., Chesterikoff, A., 1995. Analysis of the Distribution of Some Polycyclic Aromatic Hydrocarbons in Sediments and Suspended Matter in the River Seine (France). Water, Air Soil Pollut. 81, 135–152. https://doi.org/10.1007/BF00477261

Pacyna, J.M., Breivik, K., Münch, J., Fudala, J., 2003. European atmospheric emissions of selected persistent organic pollutants, 1970–1995. Atmos. Environ. 37, 119–131. https://doi.org/10.1016/S1352-2310(03)00240-1

Rocher, V., Azimi, S., Gasperi, J., Beuvin, L., Muller, M., Moilleron, R., Chebbo, G., 2004. Hydrocarbons and metals in atmospheric deposition and roof runoff in central Paris. Water. Air. Soil Pollut. 159, 67–86. https://doi.org/10.1023/B:WATE.0000049165.12410.98

Rodenburg, L.A., Valle, S.N., Panero, M.A., Muñoz, G.R., Shor, L.M., 2010. Mass Balances on Selected Polycyclic Aromatic Hydrocarbons in the New York–New Jersey Harbor. J. Environ. Qual. 39, 642. https://doi.org/10.2134/jeq2009.0264

Rose, N.L., Rippey, B., 2002. The historical record of PAH, PCB, trace metal and fly-ash particle deposition at a remote lake in north-west Scotland. Environ. Pollut. 117, 121–132. https://doi.org/10.1016/S0269-7491(01)00149-X

Schwientek, M., Rügner, H., Beckingham, B., Kuch, B., Grathwohl, P., 2013. Integrated monitoring of particle associated transport of PAHs in contrasting catchments. Environ. Pollut. 172, 155–162. https://doi.org/10.1016/j.envpol.2012.09.004

Schwientek, M., Rügner, H., Scherer, U., Rode, M., Grathwohl, P., 2017. A parsimonious approach to estimate PAH concentrations in river sediments of anthropogenically impacted watersheds. Sci. Total Environ. 601–602, 636–645. https://doi.org/10.1016/j.scitotenv.2017.05.208

Shi, Z., Tao, S., Pan, B., Liu, W.X., Shen, W.R., 2007. Partitioning and source diagnostics of polycyclic aromatic hydrocarbons in rivers in Tianjin, China. Environ. Pollut. 146, 492–500. https://doi.org/10.1016/j.envpol.2006.07.009

Sicre, M.-A., Fernandes, M.B., Pont, D., 2008. Poly-aromatic hydrocarbon (PAH) inputs from the Rhône River to the Mediterranean Sea in relation with the hydrological cycle: Impact of floods. Mar. Pollut. Bull. 56, 1935–1942. https://doi.org/10.1016/j.marpolbul.2008.07.015

Sofowote, U.M., Hung, H., Rastogi, A.K., Westgate, J.N., Deluca, P.F., Su, Y., McCarry, B.E., 2011. Assessing the long-range transport of PAH to a sub-Arctic site using positive matrix factorization and potential source contribution function. Atmos. Environ. 45, 967–976. https://doi.org/10.1016/j.atmosenv.2010.11.005

Uher, E., Mirande-Bret, C., Gourlay-Francé, C., 2016. Assessing the relation between

anthropogenic pressure and PAH concentrations in surface water in the Seine River basin using multivariate analysis. Sci. Total Environ. 557–558, 551–561. https://doi.org/10.1016/j.scitotenv.2016.03.118

Van Metre, P.C., Mahler, B.J., Furlong, E.T., 2000. Urban Sprawl Leaves Its PAH Signature. Environ. Sci. Technol. 34, 4064–4070. https://doi.org/10.1021/es991007n

Walsh, C.J., Roy, A.H., Feminella, J.W., Cottingham, P.D., Groffman, P.M., Morgan, R.P., 2005. The urban stream syndrome: current knowledge and the search for a cure. J. North Am. Benthol. Soc. 24, 706–723. https://doi.org/10.1899/04-028.1

Yunker, M.B., Macdonald, R.W., Fowler, B.R., Cretney, W.J., Dallimore, S.R., McLaughlin, F.A., 1991. Geochemistry and fluxes of hydrocarbons to the Beaufort Sea shelf: A multivariate comparison of fluvial inputs and coastal erosion of peat using principal components analysis. Geochim. Cosmochim. Acta 55, 255–273. https://doi.org/10.1016/0016-7037(91)90416-3

Table captions:

Table 1: Comparison of total PAH atmospheric fallout in the Orge River catchment (this study) with those values reported in the literature

Table 2: Comparison of Orge River PAH contamination in the particulate and dissolved phases (this study) with those values reported in previous studies conducted in France and Europe

Table 3: Comparison of subcatchment contributions to water discharge at the outlet and particulate PAH export with respect to their respective surfaces

Table 4: Specific particulate fluxes of PAH in g km^{-2} y^{-1} and specific sediment yields in t km^{-2} y^{-1} for contrasting catchments across the world

Table 1: Atmospheric deposition under each land use and corresponding PAH stock in the Orge River catchment

Table1

Click here to download Table: Table_1.docx

Location	Type	Atmospheric deposition ($\mu g\ m^{-2}\ y^{-1}$)		Reference
Orsay - France	Peri-urban	182	∑13PAHs	This study
Paris - France	Urban	57 - 472	∑14PAHs	(Garban et al., 2002)
	Urban	119		(Blanchard et al., 2007)
Créteil (Paris suburb) - France	Urban	153	∑13PAHs	(Azimi et al., 2005)
Orgeval - France	Rural	157		(Gateuille et al., 2014a)
Le Havre - France	Urban	70		(Motelay-Massei et al., 2003)
Southern Germany	Rural	200	∑17PAHs	(Gocht et al., 2007)
Northern Spain	Rural (National Park)	14 - 189	∑14PAHs	(Foan et al., 2015)

Table2

Click here to download Table: Table_2.docx

Location	Location	PAH concentration in SPM	PAH concentration in the dissolved phase		References
		µg g^{-1}	ng L^{-1}		
Orge River (France)	Peri-urban/Urban	4.6 (1-45.2)	41 (11-221)	∑13PAHs	This study
Orgeval River (France)	Rural	4.0 (0.05-14)	72 (60-112)	∑13PAHs	(Gateuille et al., 2014a)
Seine River (France)	Urban	5.8 (2.8-8.7)	80 (26-166)	∑16PAHs	(Ollivon et al., 1995)
Moselle River (France)	Industrial	4.5 (2.3-7.7)	-	∑16PAHs	(Le Meur et al., 2017)
Rhône River (France)	Urban	2.3 (0.02-7)	11 (3-89)	∑14PAHs	(Sicre et al., 2008)
Körsch River (Germany)	Urban	4.6	29	∑15PAHs	(Schwientek et al., 2013)
Elbe River (Germany)	Urban	4.7 (2.5-8.9)	-	∑16PAHs	(Heemken et al., 2000)
Mackenzie River (Canada)	Rural	2.1 ± 0.4	-	∑16PAHs	(Yunker et al., 1991)

Table3

Click here to download Table: Table_3.docx

Subcatchments		Egly	Yvette	$Viry_{sub}$
Proportion of the total catchment surface (%)		50	20	30
Proportion of the total water discharge (%)		52 ± 3	28 ± 3	21 ± 4
Specific sediment yield (t km^{-2} y^{-1})		4.2	7.1	3.1
Proportion of the total sediment load (%)		48	30	22
Particulate PAH export by each subcatchment in g d^{-1} (proportion of the total export in %)	January 2016	9.9 (32%)	1.5 (5%)	18.9 (62%)
	April 2016	14.4 (32%)	6.9 (15%)	23.9 (53%)
	August 2016	7.0 (111%)	3.4 (54%)	- 4.0 (- 65%)
	November 2016	5.4 (19%)	5.2 (19%)	17.0 (62%)

Table4

Click here to download Table: Table_4.docx

Location		Type	PAH specific load (g $km^{-2}.y^{-1}$)	Specific sediment yield (t km^{-2} y^{-1})	Ratio PAH specific load/specific sediment yield (g t^{-1})	Reference
Orge River catchment (France)	Dourdan	Rural	10.3 ± 1.1	7.4	1.4	This study
	Egly	Rural/Suburban	19.1 ± 1.0	4.2	4.5	
	Yvette	Rural/Suburban	24.8 ± 0.7	7.1	3.5	
	$Viry_{sub}$	Urban	46.7 ± 2.5	3.1	15.1	
	Viry (outlet)	Urban	28.7 ± 0.1	4.4	6.5	
Sucy (France)		Urban	1200	70	17	(Hannouche et al., 2017)
Orgeval River catchment (France)		Rural	0.2-30.4	18.9	1.6	(Gateuille et al., 2014a)
Seine River catchment (France)		Urban	70	12*	5.8	(Ollivon et al., 1995) (*Delmas et al., 2012)
Moselle River (France)		Urban/industrial	13.1	2.9	4.5	(Le Meur et al., 2017)
Rhône River (France)		Mixed	170	76	2.2	(Sicre et al., 2008)
Körsh River (Germany)		Urban	161	35	4.6	(Schwientek et al., 2013)
Elbe River (Germany)		Urban	28.5	5.3	5.4	(Heemken et al., 2000)
Mackenzie River (Canada)		Rural (Forest)	27	29	0.7	(Yunker et al., 1991)

Table5

Click here to download Table: Table_5.docx

	Agricultural soils	Forest soils	Urban soils
Atmospheric deposition (kg y^{-1})	74 ± 10	53 ± 10	46 ± 10
PAH stock (tons)	840	75	309
(min-max)	(14-4511)	(13-138)	(7-2801)

Figure captions

Figure 1: Land uses in the Orge River catchment (source: Corine Land Cover, 2012) and locations of atmospheric fallout and river monitoring stations.

Figure 2: River flow and precipitation recorded in the Orge River catchment from January to December 2016. Low flow periods (orange): August 2016 (08/24/2016-08/29/2016). Average discharge conditions (green): January 2016 (01/21/2016-01/25/2016), November 2016 (11/16/2016-11/22/2016) and December 2016 (12/05/2016, 12/15/2016 and 01/03/2017). High flow period (blue): April 2016 (04/07/2016-04/11/2016). Extreme flood (black): June 2016 (06/06/2016: water flow decrease).

Figure 3: Spatial and temporal variations of dissolved PAH proportions (a, b), temporal variations of PAH dissolved concentrations in ng L-1 (c) and spatial variation of particulate contents in µg g-1 (d). Significant differences between groups (sites or campaigns) are represented by (*)

Figure 4: Riverine export of PAH in the dissolved phase (a) and the particulate phase (b) for different sampling campaigns conducted in the Orge River in 2016

Figure 1: Annual mass balance of total PAH fluxes (dissolved and particulate) estimated for the Orge River catchment and the subcatchments of Egly, Yvette, Dourdan and Virysub associated with PAH atmospheric deposition and the annual accumulation rate for each subcatchment

Figure1

Click here to download high resolution image

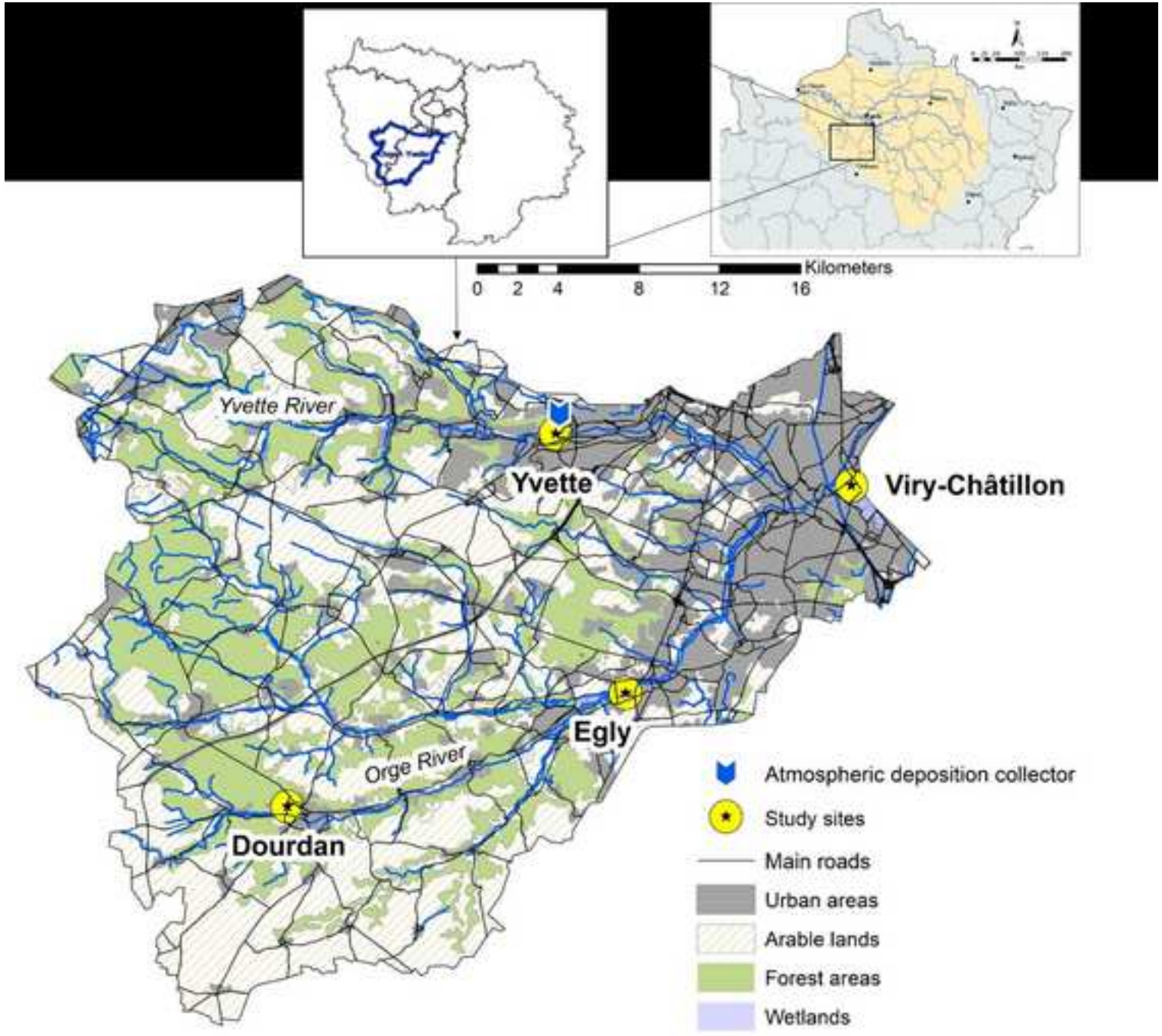

Figure2

Click here to download high resolution image

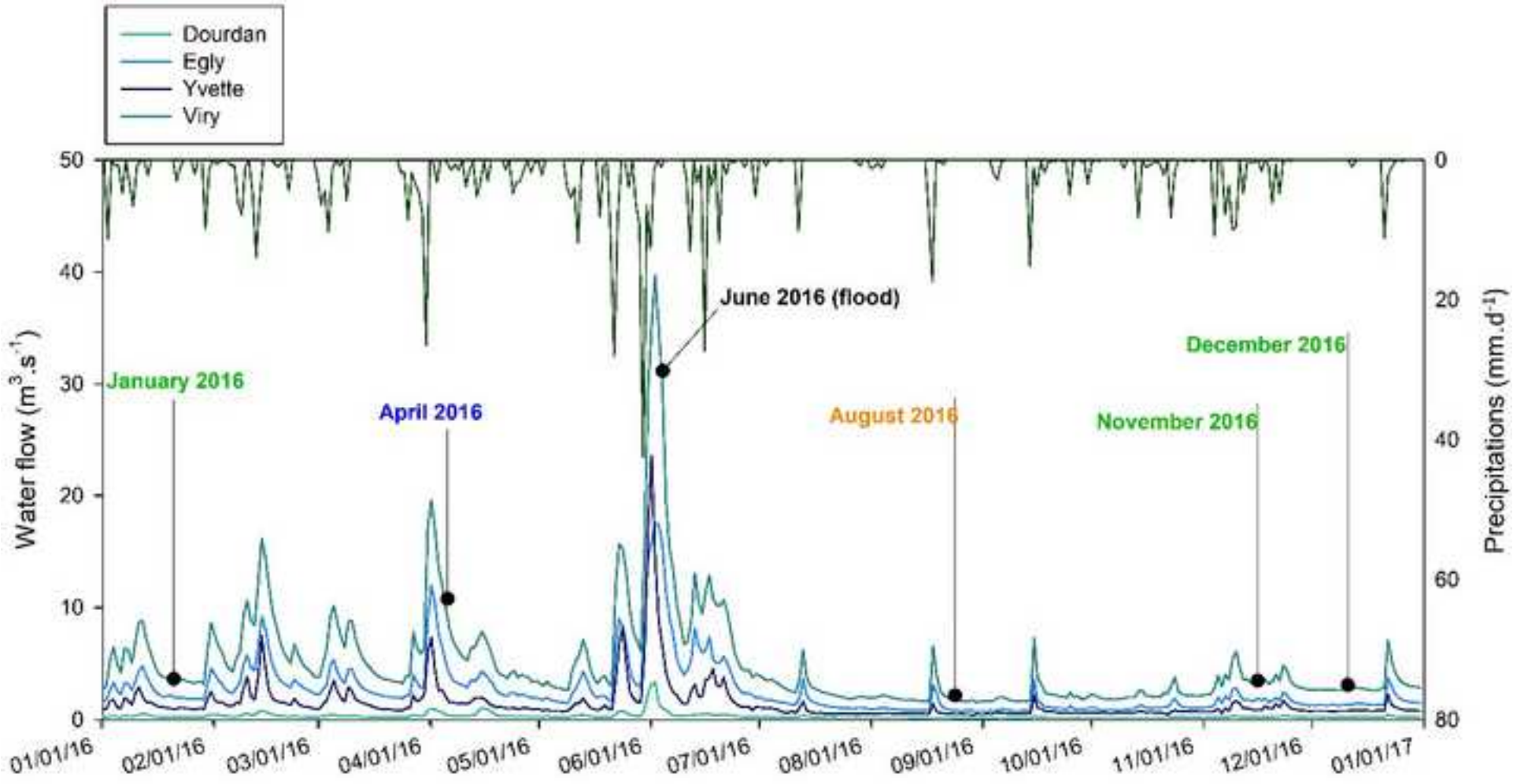

Figure3

Click here to download high resolution image

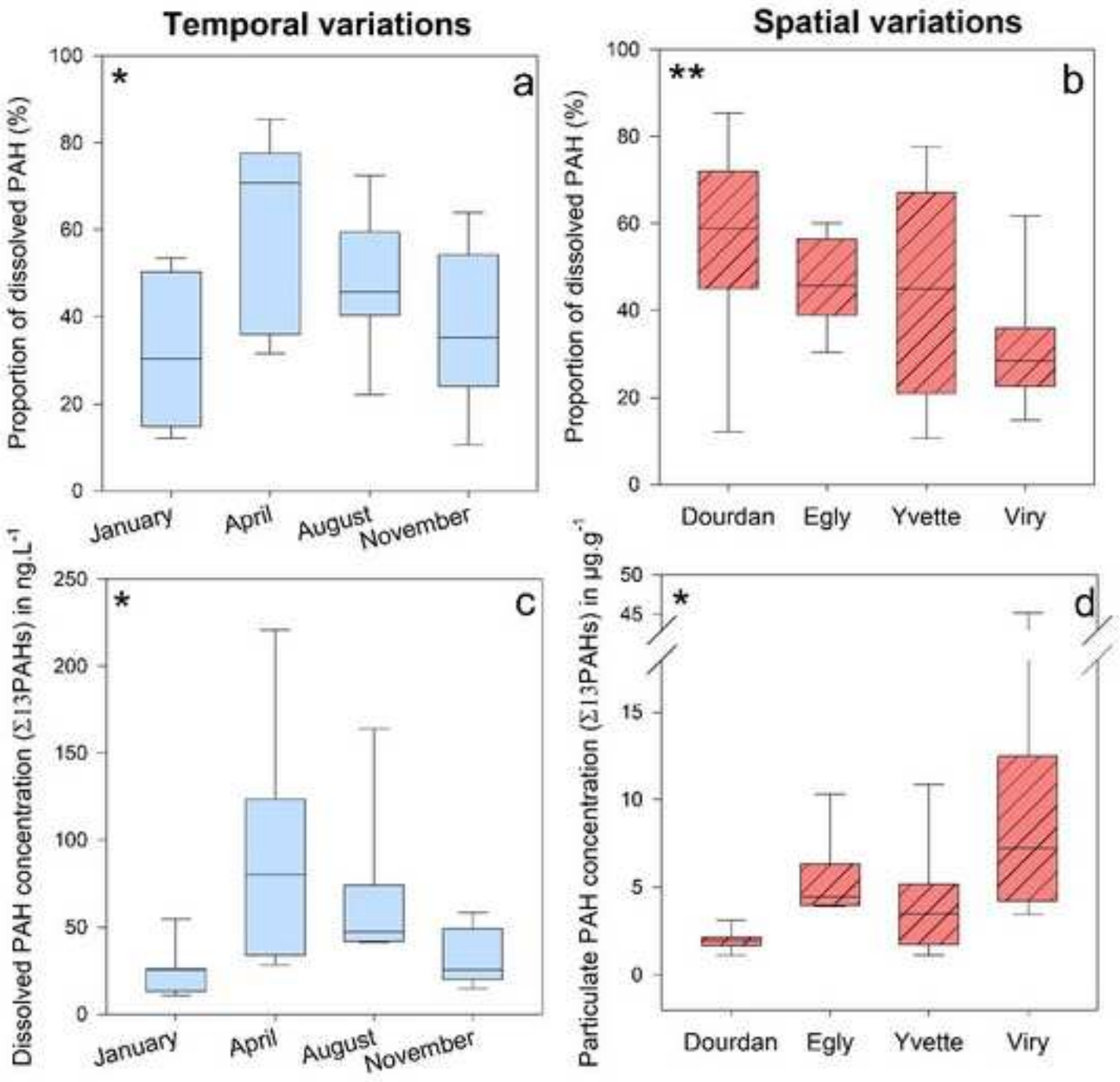

Figure4

Click here to download high resolution image

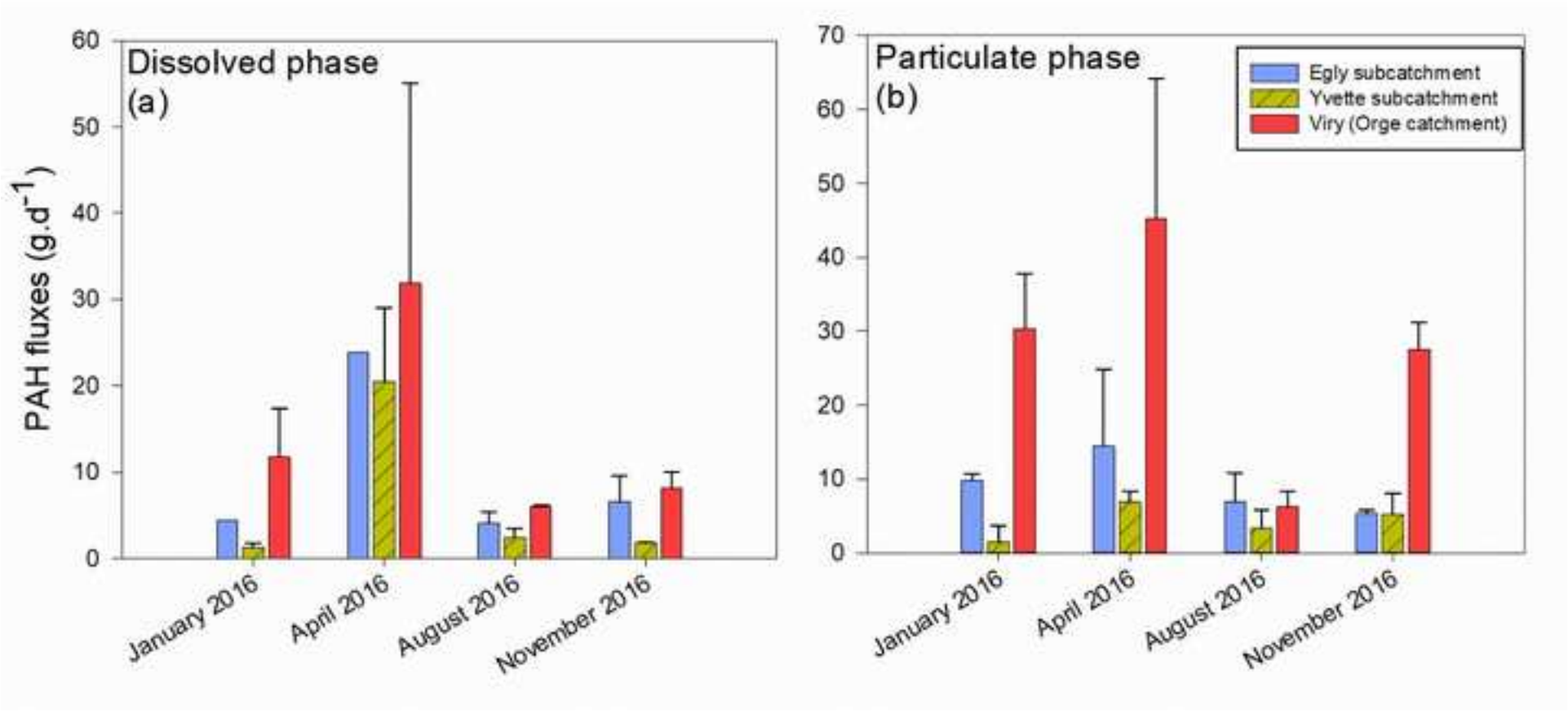

Figure5

Click here to download high resolution image

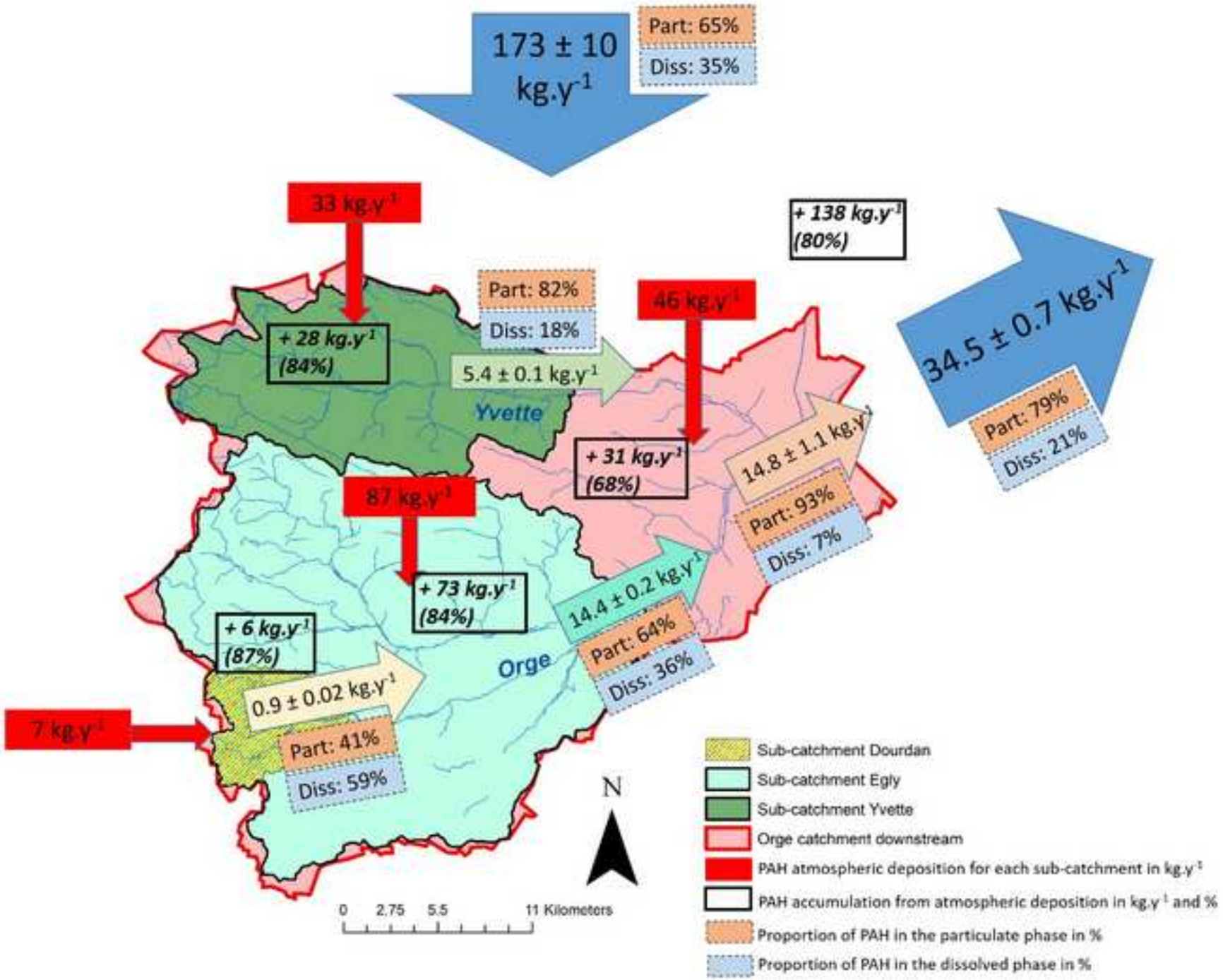

Supplementary Material

Click here to download Supplementary Material: Froger_Supplementary_material_revision1_VF.docx